

Supplementary Materials

Table of Contents

List of Supplementary Figures	1
List of Supplementary Tables	1
Supplementary Methods and Analyses	3
Detailed methods for new MA lines (Assaf), and meta-analysis of 5 experiments	3
Pipeline and analyses for identification/validation of extremely rare singletons . .	6
Codon usage does not affect expected nonsynonymous and nonsense fraction . . .	9
Investigating the ‘missing’ fraction of nonsynonymous and nonsense mutations .	9

List of Supplementary Figures

Supplemental Fig S1	Rare polymorphisms: Identification	14
Supplemental Fig S2	Rare polymorphisms: Quality metrics	15
Supplemental Fig S3	Rare polymorphisms: Distance distribution	16
Supplemental Fig S4	MA (Assaf): Sequencing coverage	17
Supplemental Fig S5	MA (Assaf): Experiment information	18
Supplemental Fig S6	All data: Distribution of phastCons scores	19
Supplemental Fig S7	All data: Heterozygous nonsense mutations	20
Supplemental Fig S8	All data: GC equilibrium and GC content	20
Supplemental Fig S9	All data: Six relative rates	21

List of Supplementary Tables

Supplemental Table S1	MA (Assaf): Experiment information	22
Supplemental Table S2	MA (Assaf): Mutation list	23
Supplemental Table S3	MA (Assaf): Sanger sequencing	24
Supplemental Table S4	MA (all): Experiment information	25
Supplemental Table S5	MA (all): Six relative rates	25
Supplemental Table S6	MA (all): Triplet context	26
Supplemental Table S7	MA (Assaf): Absolute mutation rates	27
Supplemental Table S8	All data: GO analysis	28
Supplemental Table S9	Rare polymorphisms: Triplet context	29
Supplemental Table S10	Evolved four-fold degenerate sites: Triplet context . . .	30

Supplementary Methods and Analyses

Detailed methods for new MA lines (Assaf), and meta-analysis of 5 experiments

Mutation accumulation experiment: Two strains are used for the experiment: DGRP strain RAL-765 (wildtype genotype $\frac{+}{+}; \frac{+}{+}; \frac{+}{+}$) which has red eyes, and a white-eyed laboratory strain $\frac{+}{Y, hshid}; \frac{bw[1]}{bw[1]}; \frac{st[1]}{st[1]}$ generated by Mark Siegal at New York University, hereafter referred to as hshid (for the ‘heat shock head involution defective’ genotype). The hshid strain allows the easy acquisition of virgins, because all males die upon one-hour heat shock during the larval stage. Using these two strains, the MA chromosomes (i.e. DGRP) are always passed through red-eyed males that are heterozygous with the hshid chromosomes, allowing the MA chromosomes to avoid recombination (because males lack it) and to never be subjected to heat-shock (because only hshid chromosomes are heat-shocked). The crosses were as follows: A single male fruit fly from DGRP strain RAL-765 was crossed with 6 virgin hshid females, after which a single red-eyed male progeny (i.e. heterozygous for both bw and st and therefore carrying the founder male’s 2nd and 3rd chromosomes) was taken and crossed to 6 hshid virgin females. From this cross, 50 red-eyed male progeny were then isolated within vials, thus founding 50 MA strains with identical chromosome 2 and 3. Thereafter every generation a single red-eyed male progeny from each strain was crossed to 3 hshid virgin females, and as backup this was replicated using male siblings in 3 additional vials each generation.

Mutation accumulation line sequencing: As is common in MA experiments, some lines became sick and died off as generations passed, such that we were able to sequence 17 lines out of the original 50. From these 17 MA strains, five to fifteen flies were taken (thus heterozygous for the MA chromosome) in generations 36, 37, 49, and 53, and DNA extracted according to a standard protocol [Huang et al. 2009]. Paired-end barcoded DNA sequencing libraries were prepared using Illumina Nextera Sample Preparation Kit (FC-121-1031) and Index Kit (FC-121-1012) and KAPA Biosystems Library Amplification Kit (KK2611), modified for small volumes. In brief: Genomic DNA was diluted to 2.5ng/uL using quantification with Qubit HS Assay Kit (Q32851), and then 1ul of DNA was ‘tagmented’ according

to the Nextera protocol in a 2.5ul total volume (55°C, 5 minutes), then each library was amplified using the KAPA amplification kit with Nextera index primers (N7XX and N5XX) in a 7.5ul total volume (98°C for 165sec, 8 cycles of 98°/62°/72° for 15sec/30sec/90sec), and then reconditioned to add Nextera PCR primers (required for Illumina sequencing) in a 17ul total volume (95°C for 5min, 4 cycles of 98°/62°/72° for 20sec/20sec/30sec). Libraries were sequenced on a HiSeq 2000 to a depth of 20-25X (see Supplementary Materials for sample coverage plot).

Mutation accumulation variant calling: In order to call *de novo* mutations in these strains heterozygous for the MA and hshid chromosomes, we sequenced the ancestral DGRP and hshid strains in addition to each MA line, and then accepted genetic variants which were strictly unique to each MA strain (thus hshid variants segregating across the heterozygous MA strains were filtered out). The following pipeline was used to call genetic variants in the MA sequencing data, where default settings for each tool were used unless otherwise specified: Reads were trimmed with TrimGalore! v0.3.7 [http://www.bioinformatics.babraham.ac.uk/projects/trim_galore] (`trim_galore -a CTGTCTCTTATACACATCT -a2 CTGTCTCTTATACACATCT --quality 20 --length 30 --clip_R1 15 --clip_R2 15 --three_prime_clip_R1 3 --three_prime_clip_R2 3 --paired`), then mapped to release 5.57 of the *Drosophila* reference genome with BWA-MEM v0.7.5a [Li 2013]. Next PCR duplicates were removed with PicardTools v1.105 [<http://broadinstitute.github.io/picard>] (`MarkDuplicates REMOVE_DUPLICATES=true`), and then reads locally rearranged around indels with GATK v3.2.2 [Van der Auwera et al. 2013] (`RealignerTargetCreator` and `IndelRealigner` tools). Variants were called with GATK (`HaplotypeCaller --heterozygosity 0.01`) followed by the GATK recommended conservative filters (`VariantFiltration --filterExpression "QD < 2.0 || FS > 60.0 || MQ < 40.0 || MQRankSum < -12.5 || ReadPosRankSum < -8.0"`), and new mutations were considered the variants present in one MA strain and absent from all the rest. Variants were also called with a less conservative pipeline using SAMtools v0.1.19 [Li et al. 2009] to generate a mpileup file (`mpileup`) followed by Varscan v2.3.9 [Koboldt et al. 2012] to call variants (`mpileup2cns --min-coverage 4 --min-reads2 2 --min-var-freq 0.01 --min-freq-for-hom 0.99 --strand-filter 0 --p-value 1`), and again new mutations were considered the variants present in one MA strain and absent

from all the rest. Repetitive regions were then filtered out, including from RepeatMasker [<http://www.repeatmasker.org>], from a run of TRF [Benson 1999] on the *Drosophila* reference, and from a list of annotated transposable elements [Fiston-Lavier et al. 2011]. The final list of new mutations was considered the intersection of the two variant call sets, in order to ensure that a new mutation was both a high quality variant call (i.e. the conservative GATK set) and also never observed in any other strain (i.e. nonconservative Varscan set). Thirty variants were amplified with PCR and then Sanger sequenced, of which twenty-nine were confirmed. A summary of the mutation counts and generations of mutation accumulation for each strain can be found in Supplementary Materials, along with a summary of the mutations randomly chosen for validation via PCR/Sanger sequencing and their corresponding primers. After masking repetitive regions, the total genome length for chromosomes 2 and 3 was 87,130,614 base pairs. The total number of MA generations (762 across all lines) was multiplied by the total number of post-filtered base pairs to get 66,393,527,868, which is the denominator for the mutation rate calculation.

MA data from references [Schridder et al. 2013; Keightley et al. 2009; Sharp and Agrawal 2016; Huang et al. 2016]: Lists of mutations from each experiment were downloaded from each publication and then processed with in-house *perl* and *R* scripts to generate a single VCF of all mutations, which is available as a supplementary file. For the ‘MA combined’ datasets, we filtered out repetitive regions (including from RepeatMasker [<http://www.repeatmasker.org>], from a run of TRF [Benson 1999] on the *Drosophila* reference, and from a list of annotated transposable elements [Fiston-Lavier et al. 2011]), removed mutator lines (line 19 from Huang et. al., and lines 33-27, 33-45, 33-5, and 33-55 from Schridder et. al.), and subsetted down to the major autosomes 2 and 3 only. For comparisons of the single base pair mutation rates with a poisson exact test we require a time base in order to scale the different experiment counts, and while the number of generations and number of lines were provided within the publications, the information on genome size was incomplete. Thus, given that mutation rate $\mu = m/(n \times t \times l)$ (where m =mutation count, n =number of strains, t = number of generations, and l = number of base pairs), we back-calculated l , which can be found in the last column of Supplementary Materials.

Pipeline and analyses for identification/validation of extremely rare singletons

As a proxy for new mutations, we seek to identify a class of ultra-low-frequency polymorphisms. To this purpose, we use three publicly available datasets and employ the method depicted in Supplemental Fig S1A and briefly described here: i) We first downloaded 621 genomes from the Drosophila Genome Nexus (DGN)[Lack et al. 2015], which represent predominantly monoallelic genomes (i.e. either haploid or inbred) from 35 populations across 3 continents that underwent the same iterative mapping pipeline before variant calling. These data represent an extremely high quality set of genotype calls, and thus we identified all genetic variants with which we will be working using these data (Step 1 in Supplemental Fig S1A). ii) We next leveraged the availability of pooled sequencing data generated by our and collaborating labs, which collectively represent >4,000 genomes from the eastern USA and Europe [Bergland et al. 2014] [plus additional unpublished data]. Pooled sequencing data is not ideal for rare variant identification, due to the difficulty of distinguishing a rare polymorphism from a sequencing error [Raineri et al. 2012]. In order to circumvent this, we used the set of high quality DGN singletons identified in Step 1, i.e. those at 1/621 frequency, and filtered them down by removing those that appeared in the pooled sequence data. This allowed the identification of DGN singletons at a frequency that is an order of magnitude lower (frequency $\sim 1/5000 = 0.0002$) (Step 2 in Supplemental Fig S1A). iii) Finally, the third public resource we leveraged is resequence data made available by the DGRP and DPGP1 projects, which independently resequenced 29 strains (present in the DGN) using Roche 454 and Illumina sequencing [unpublished but available online]. Given that any pipeline which filters down to polymorphisms unique to a single genome is likely to be enriching for sequencing error (i.e. a polymorphism segregating in multiple individuals or multiple datasets is less likely to be an error), we further validated our rare DGN variants by requiring an identical genotype call to be made in the resequence data (Step 3 in Supplemental Fig S1A). This procedure does reduce the number of polymorphisms down to only those which appeared in the 29 resequenced strains, however this dataset is of extremely high quality.

This procedure confirms that, indeed, the proportion of artifactual variants increases as their frequency decreases (Supplemental Fig S1B-D), and as a consequence it is absolutely critical to validate rare variants using resequence data. We find that while common DGN variants are confirmed in the resequence data at a rate close to $\sim 100\%$, the rarest DGN variants, at frequency $\sim 1/5000$, have a much lower confirmation rate in the resequence data of $<60\%$ (Supplemental Fig S1B, green points). We find this to be primarily driven by sites that are not genotyped at all during resequencing, due to the fact that if we look at only DGN variants which were successfully genotyped in the resequence data, we find the confirmation rate rises back to $\sim 100\%$ (Supplemental Fig S1B, purple points). This low confirmation rate for rare polymorphisms appears to be largely driven by low complexity and indel-rich regions (Supplemental Fig S1C-D). As can be seen in Supplemental Fig S1C, rarer DGN polymorphisms have a lower confirmation rate in intronic and intergenic regions (Supplemental Fig S1C, left and center panels), an effect which is negligible for common variants (Supplemental Fig S1C, right panel), and which disappears when looking at only DGN variants with a genotype call in the resequence data (Supplemental Fig S1C, purple points). As can be seen in Supplemental Fig S1D, despite masking each DGN genome for indels before calling variants in that individual (Methods), rare DGN variants have a low confirmation rate within sites at which indels are segregating in other individuals (Supplemental Fig S1D, left and center), an effect that is exacerbated as the indel frequency (i.e. copy count) increases in the DGN population. This effect is again negligible for common variants (Supplemental Fig S1D, right panel), and disappears when looking at only DGN variants with a genotype call in the resequence data (Supplemental Fig S1D, purple points).

These results beg the question of whether more severe filtering can approximate the quality-control achieved with resequencing, i.e. does the confirmation rate recover if we filter down to DGN genotype calls which have better scores for metrics like depth and quality score? To ask this we measured confirmation rate after implementing standard filters used by most researchers (site has $QUAL > 20$, $QD > 2$, $3 > DP > 100$ (note mean depth of data is $\sim 25X$)), as well as much more severe filters (site has $QD > 3$, $QUAL > 55$, $9 > DP > 100$, genotype data in $\geq 85\%$ of samples, indels in ≤ 10 samples). As can be seen in Supplemental Fig S1E, the standard filters used by many researchers give rare

polymorphisms that still have a confirmation rate as low as $\sim 70\%$, and while severe filters do better at a $\sim 90\%$ confirmation rate, this rate is not ideal given that a tenth of the data may still be error-prone. These results make sense if we look at the distribution of DP and QUAL scores within the DGN data for sites that are confirmed, disconfirmed, and ungenotyped in the resequence data. While the distributions of scores are significantly different, they also overlap (Supplemental Fig S2), and thus even severe filters are likely to let through variant calls that may be errors. These results emphasize the importance of resequencing genomes when working with polymorphisms that are segregating at low frequency. The final count of rare polymorphisms that we will use in this study, all confirmed via resequencing, can be seen in the main text.

The reduced confirmation rate within introns and intergenic regions, as well as near indels, emphasizes the difficulty of validating rare polymorphisms within low-complexity regions. It has been observed before that artifactual variant calls in high-coverage sequencing samples are largely driven by alignment errors [Li 2014]. This is potentially worrisome when testing for mutational biases in the genome, because some tests rely inherently on our ability to ‘count the reference’, meaning accurately quantifying in the reference genome the relative proportions of sequence contexts in which we might be interested. For example, it is known that both AT-rich and GC-rich genomic regions are underrepresented in sequencing data [Dohm et al. 2008; Benjamini and Speed 2012], such that GC balanced regions of the genome with better read coverage may have a higher discovery rate of genetic variants. Thus, even when we are confident our genetic variants are real, when working with rare polymorphisms we must be careful not to confound intrinsic rates of detection with intrinsic rates of mutation. For this reason, when using metrics which rely on quantifying relative proportions of sequence context in the reference genome (e.g. six relative rates), we prefer to work with higher complexity zones such as coding regions, or alternatively re-frame the metric in such a way as to not be sensitive to this factor. We note that a similar approach is used in other studies of context-dependent mutational patterns [Aggarwala and Voight 2016], and that while our results are robust to this choice we consider it to be the more conservative approach.

Codon usage in *D. melanogaster* and how it affects the expected fraction of nonsynonymous and nonsense mutations in coding regions

Consider that there are 61 amino acid codons * 3 sites per codon * 3 mutations that can occur per site, this means there are a total of 549 possible codon mutations. There are:

- 2 amino acids with 1 codon only, such that there are 0 possible synonymous mutations
- 9 aa with 2 codons, thus 2 possible synonymous mutations per amino acid
- 1 aa with 3 codons, thus 6 possible synonymous mutations per amino acid
- 5 aa with 4 codons, thus 12 possible synonymous mutations per amino acid
- 3 aa with 6 codons, and 20 possible synonymous mutations per amino acid
- 3 aa with 6 codons, and 20 possible synonymous mutations per amino acid

This means that there are a total of $(9*2+1*6+5*12+3*20)=144$ possible synonymous mutations out of 549 possible mutations total, or in other words 73.8% probability that mutations are nonsynonymous (if you include stop codons in the denominator then this value is 75% exactly). If you scale the 61 amino acid codons using the codon usage in *D.mel* this changes to a 74.7% probability of a nonsynonymous mutation (which doesn't significantly change with the addition of stop codons, since there are so few). This calculation is using the codon usage table available from <http://www.kazusa.or.jp>

If you do the same calculation for nonsense mutations, but now include stop codons, you get 23 possible nonsense mutations out of $64*3*3=576$ possible mutations total, or in other words a 3.99% probability that mutations are nonsense. If you scale this by codon usage this changes to 3.97% of mutations.

Investigating the 'missing' fraction of nonsynonymous and nonsense mutations

Rare polymorphisms indeed approach the neutral expectation, however there remains a small 'missing' fraction of deleterious events, presumably because natural selection is efficient enough to remove them even at rare frequencies. One possible explanation is that

these missing nonsynonymous and nonsense mutations are recessive lethals, and thus potentially underrepresented in our set of resequenced rare polymorphisms. This could occur because the resequenced lines were exclusively inbred strains, and thus recessive lethals either removed via purifying selection during the inbreeding process, or lying within regions enriched for recessive lethals in repulsion (and thus masked in the final genotype calls by virtue of appearing in residually heterozygous regions). To test the second possibility we went back to the DGN raw genotype calls and pulled out singletons occurring in a heterozygous state that were also confirmed in the re-sequencing data. We found that, even in this dataset, there are only $\sim 1\%$ nonsense changes and $\sim 60\%$ nonsynonymous changes within coding regions (Supplemental Fig S7), suggesting that balanced recessive lethals are not a substantial fraction of the missing deleterious mutations. This however does not preclude the possibility that the inbreeding process permitted strongly deleterious recessive alleles to be purged from the genome [Charlesworth and Willis 2009].

Lastly, we can gain insight into which biological features are most susceptible to the deleterious effects of mutation by performing a GO analysis. Consider that sites susceptible to deleterious events are expected to be over-represented in conserved sites and under-represented among common polymorphisms. Indeed, by performing these tests for over- and under-represented terms, we find similar sets of GO terms across all analyses (Supplemental Table S8) (note that our analysis of over-represented terms within conserved sites gave similar results to a previous study [Siepel et al. 2005]). The 5 GO terms which came out in our analyses included: chromatin assembly or disassembly, cytosol, nucleosome, nucleosome assembly, and protein heterodimerization activity.

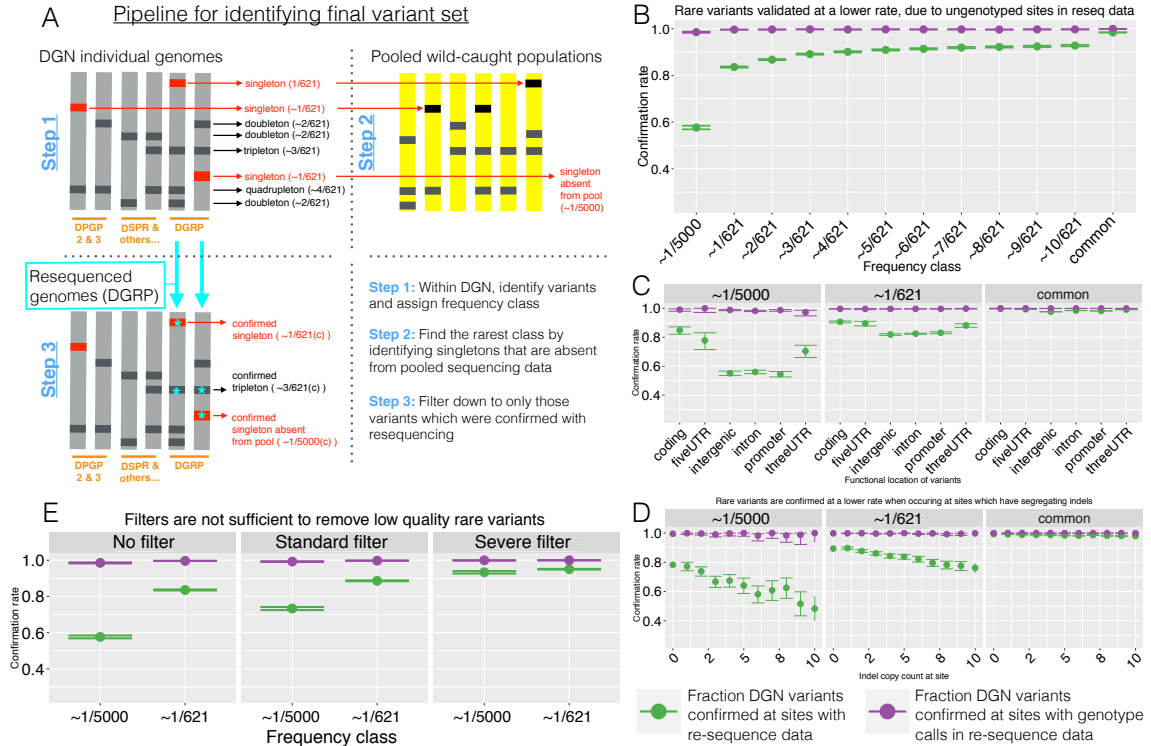
References

- Aggarwala, V. and Voight, B. F. (2016). An expanded sequence context model broadly explains variability in polymorphism levels across the human genome. *Nature Genetics*, (April 2015):1–10.
- Benjamini, Y. and Speed, T. P. (2012). Summarizing and correcting the GC content bias

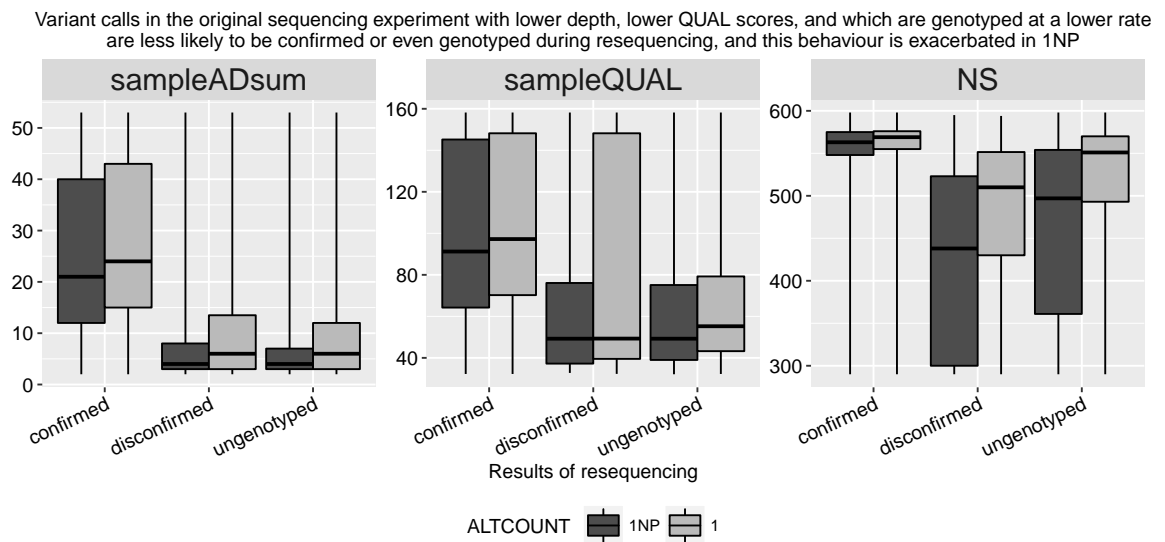
- in high-throughput sequencing. 40(10):1–14.
- Benson, G. (1999). Tandem repeats finder: A program to analyze DNA sequences. *Nucleic Acids Research*, 27(2):573–580.
- Bergland, A. O., Behrman, E. L., O’Brien, K. R., Schmidt, P. S., and Petrov, D. a. (2014). Genomic Evidence of Rapid and Stable Adaptive Oscillations over Seasonal Time Scales in *Drosophila*. *PLoS Genetics*, 10(11):e1004775.
- Charlesworth, D. and Willis, J. H. (2009). The genetics of inbreeding depression. *Nature reviews. Genetics*, 10(11):783–96.
- Dohm, J. C., Lottaz, C., Borodina, T., and Himmelbauer, H. (2008). Substantial biases in ultra-short read data sets from high-throughput DNA sequencing. *Nucleic Acids Research*, 36(16).
- Fiston-Lavier, A.-S., Carrigan, M., Petrov, D. A., and González, J. (2011). T-lex: a program for fast and accurate assessment of transposable element presence using next-generation sequencing data. *Nucleic acids research*, 39(6):e36.
- Huang, A. M., Rehm, E. J., and Rubin, G. M. (2009). Quick preparation of genomic DNA from *Drosophila*. *Cold Spring Harbor Protocols*, 4(4):10–12.
- Huang, W., Lyman, R. F., Lyman, R., Carbone, M. A., Harbison, S., Magwire, M., and Mackay, T. F. C. (2016). Spontaneous Mutations and the Origin and Maintenance of Quantitative Genetic Variation. *eLife*, 5(e14625):1–23.
- Keightley, P. D., Trivedi, U., Thomson, M., Oliver, F., Kumar, S., and Blaxter, M. L. (2009). Analysis of the genome sequences of three *Drosophila melanogaster* spontaneous mutation accumulation lines: Supplementary Tables and Figure. *Genome research*, 19:1–8.
- Koboldt, D. C., Zhang, Q., Larson, D. E., Shen, D., Mclellan, M. D., Lin, L., Miller, C. a., Mardis, E. R., Ding, L., and Wilson, R. K. (2012). VarScan 2 : Somatic mutation and copy number alteration discovery in cancer by exome sequencing VarScan 2 : Somatic

- mutation and copy number alteration discovery in cancer by exome sequencing. *Genome Research*, 22(3):568–576.
- Lack, J. B., Taylor, W., Stevens, K. A., Pool, J. E., Langley, C. H., Cardeno, C. M., Crepeau, M. W., and Corbett-Detig, R. B. (2015). The *Drosophila* Genome Nexus: a population genomic resource of 623 *Drosophila melanogaster* genomes, including 197 from a single ancestral range population. *Genetics*.
- Li, H. (2013). Aligning sequence reads, clone sequences and assembly contigs with BWA-MEM. *arXiv preprint arXiv*, 00(00):3.
- Li, H. (2014). Towards Better Understanding of Artifacts in Variant Calling from High-Coverage Samples. pages 1–8.
- Li, H., Handsaker, B., Wysoker, A., Fennell, T., Ruan, J., Homer, N., Marth, G., Abecasis, G., and Durbin, R. (2009). The Sequence Alignment/Map format and SAMtools. *Bioinformatics*, 25(16):2078–2079.
- Raineri, E., Ferretti, L., Esteve-Codina, A., Nevado, B., Heath, S., and Pérez-Enciso, M. (2012). SNP calling by sequencing pooled samples. *BMC Bioinformatics*, 13(1):239.
- Schrider, D. R., Houle, D., Lynch, M., and Hahn, M. W. (2013). Rates and genomic consequences of spontaneous mutational events in *Drosophila melanogaster*. *Genetics*, 194(4):937–54.
- Sharp, N. P. and Agrawal, A. F. (2016). Low Genetic Quality Alters Key Dimensions of the Mutational Spectrum. *PLoS biology*, 14(3):e1002419.
- Siepel, A., Bejerano, G., Pedersen, J. S., Hinrichs, A. S., Hou, M., Rosenbloom, K., Clawson, H., Spieth, J., Hillier, L. W., Richards, S., Weinstock, G. M., Wilson, R. K., Gibbs, R. a., Kent, W. J., Miller, W., and Haussler, D. (2005). Evolutionarily conserved elements in vertebrate, insect, worm, and yeast genomes. *Genome Research*, 15:1034–1050.
- Van der Auwera, G. A., Carneiro, M. O., Hartl, C., Poplin, R., del Angel, G., Levy-Moonshine, A., Jordan, T., Shakir, K., Roazen, D., Thibault, J., Banks, E., Garimella,

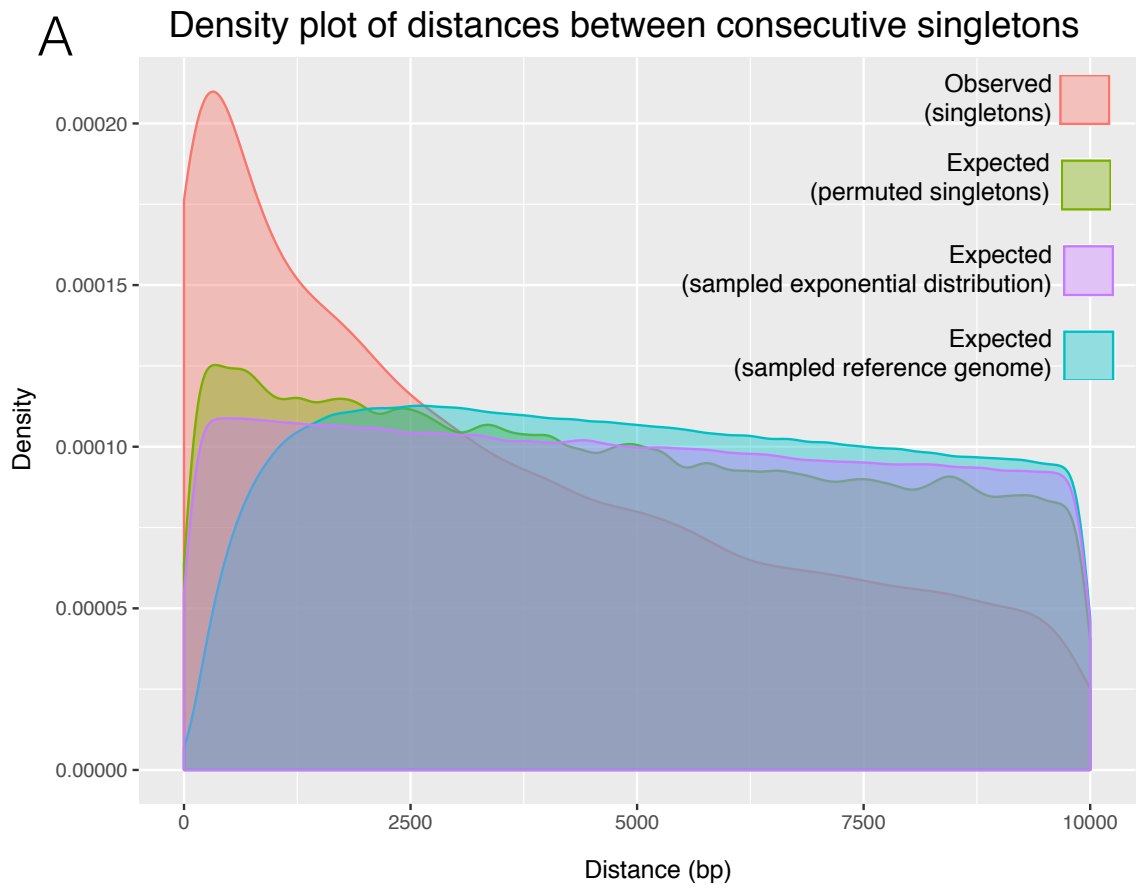
K. V., Altshuler, D., Gabriel, S., and DePristo, M. A. (2013). From fastQ data to high-confidence variant calls: The genome analysis toolkit best practices pipeline. *Current Protocols in Bioinformatics*, 11.10(SUPL.43):1–33.



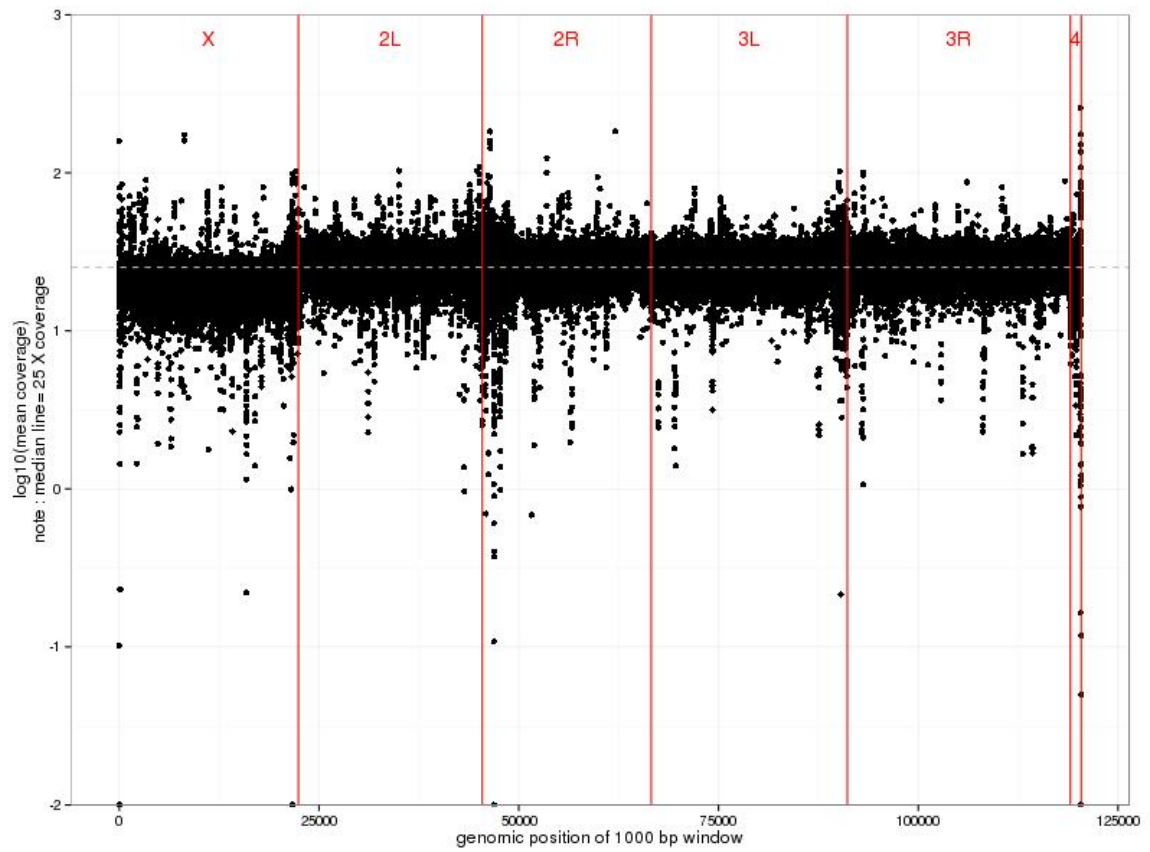
Supplemental Fig S1: Description of the data pipeline and quality used in the identification of low frequency polymorphisms. (A) Diagram of Steps 1 thru 3 in identifying a high quality set of rare polymorphisms, (B)-(E) depict confirmation rate where **green** indicates the fraction of genotype calls within the DGN data (identified in Step 1) which were confirmed in the resequence data (Step 3), and **purple** indicates the fraction of genotype calls within the DGN data which were not disconfirmed (i.e. using polymorphisms for which a genotype call exists in both the DGN and resequence data to measure the confirmation rate). The confirmation rate is depicted as a function of (B) frequency, (C) of genomic location, (D) of segregating indel copy number, and (E) of the filters applied to the dataset. For (E) the filters include no filters, standard filters (QD > 2, QUAL > 20, and 3>DP>100), and severe filters (QD > 3, QUAL > 55, and 9>DP>100, and requiring that each genotype call is at a site for which 85% of individuals have a genotype call and for which the total copy number of indels segregating in other individuals is ≤ 10).



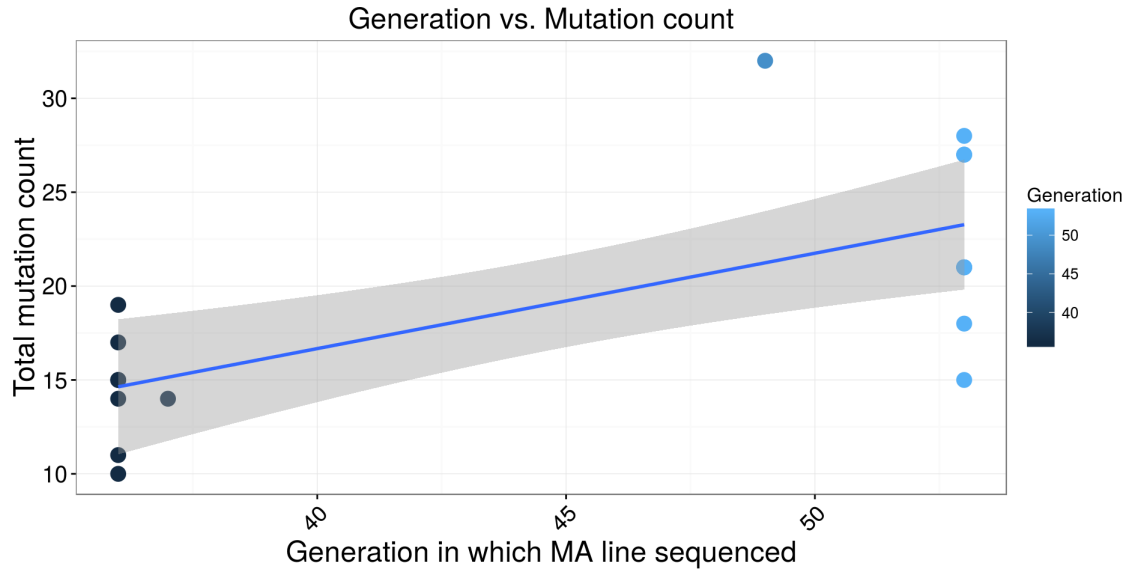
Supplemental Fig S2: Quantifying the DGN quality metrics of the DGN variants (1NP and 1 refer to variants at frequency $\sim 1/5000$ and $\sim 1/621$ respectively) after classifying them by whether in the resequence data the DGN variants were confirmed, disconfirmed, or ungenotyped. Left panel is the total depth at the site in the DGN data, middle is the QUAL score of the genotype call in the DGN data, and right panel is the number of samples with genotype information in the DGN data. DGN variants which were confirmed in the resequence data consistently have higher quality metrics, however there is also overlap in the distribution of DGN quality scores (i.e. DP, QUAL, NS) between those variants which were confirmed, disconfirmed, and ungenotyped in the resequence data.



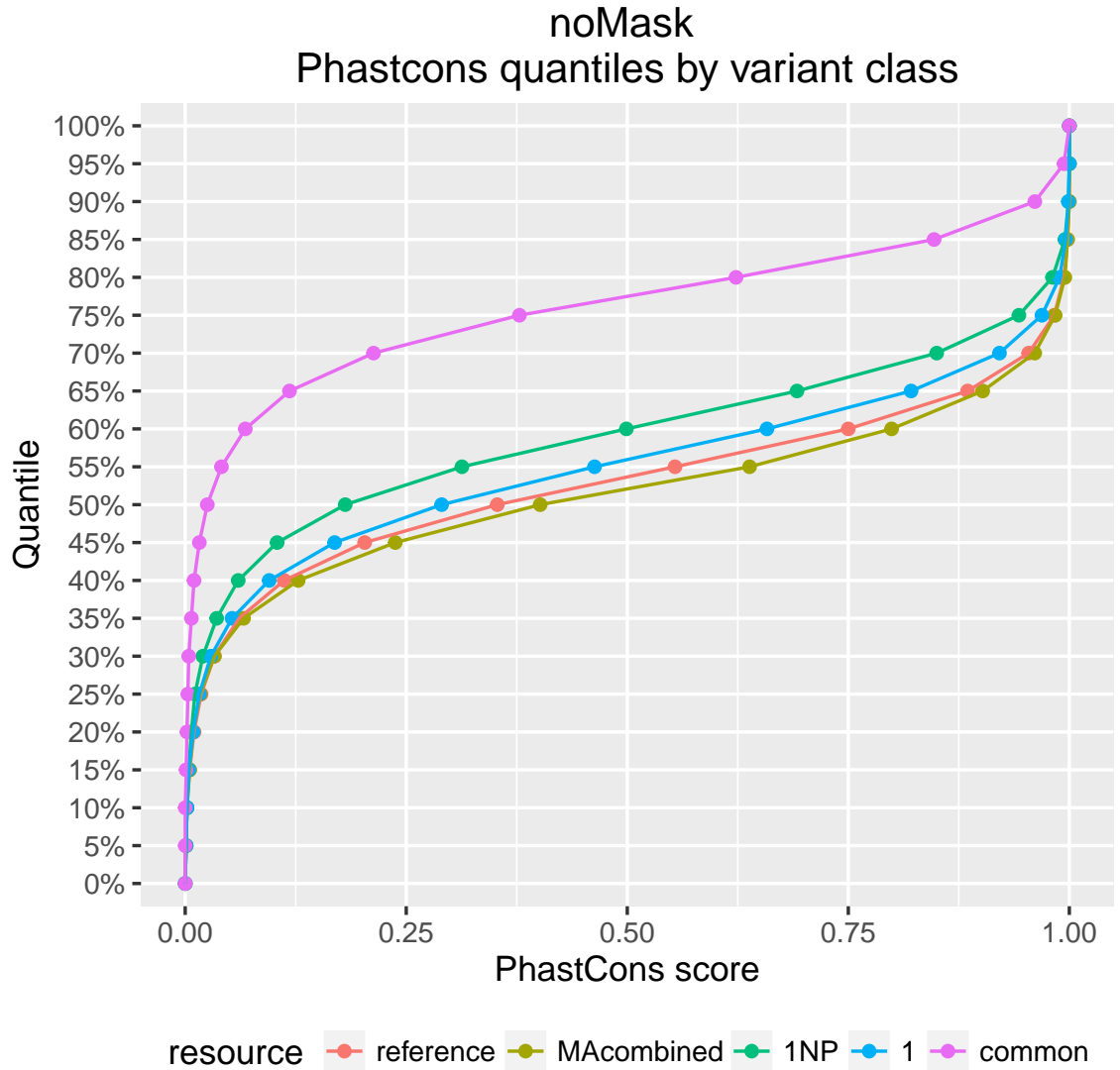
Supplemental Fig S3: Density plots of sample data, and various possible expected distributions



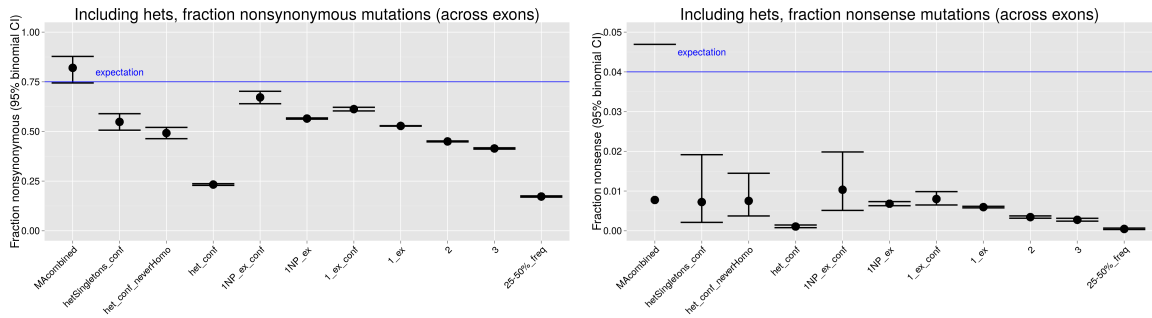
Supplemental Fig S4: Representative example of the coverage achieved across the genome for a given MA line in this study, here from MA line 33 with a median coverage of 25X.



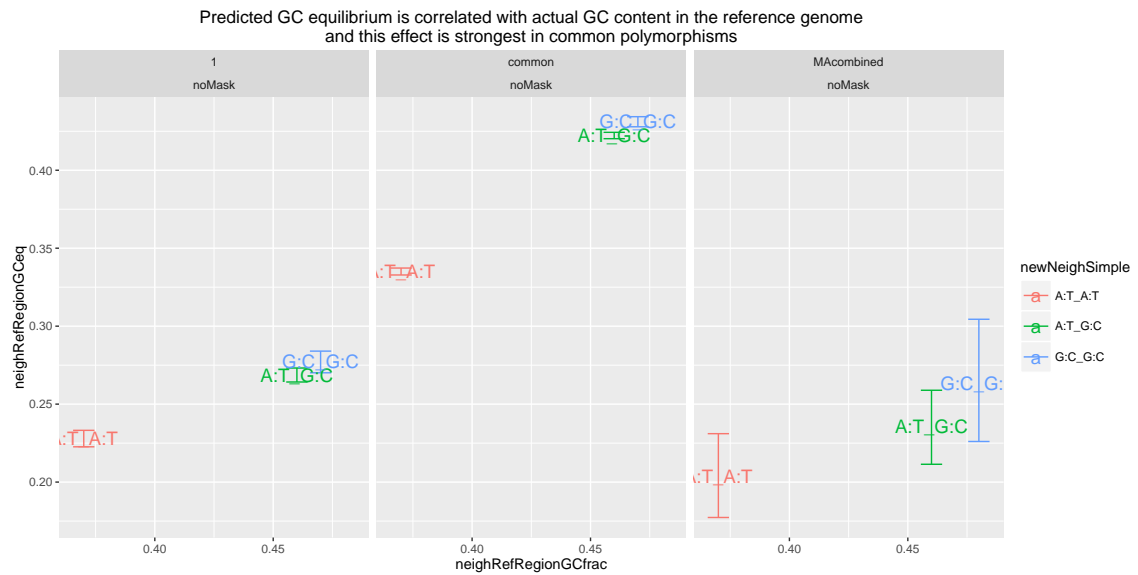
Supplemental Fig S5: A plot of the total count of mutations on each chromosomal arm for each strain as a function of generation time in which sequenced. There was no significant difference in the rates between the generations, Poisson exact test p-value = 0.757.



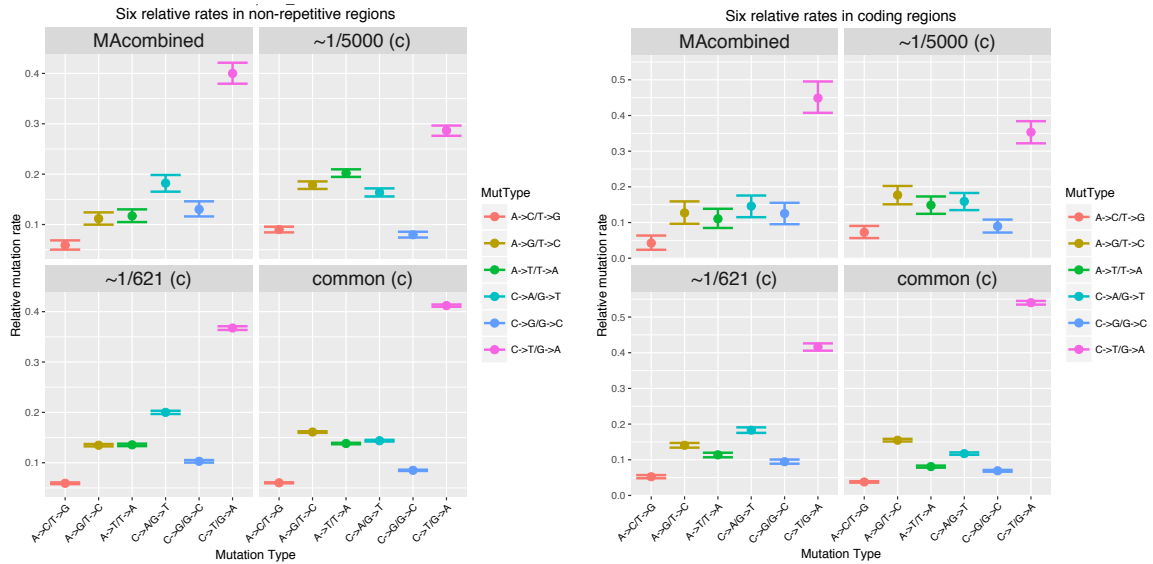
Supplemental Fig S6: The empirical cumulative distribution of phastCons scores for different classes of polymorphisms, and the reference genome. Recalling that phastCons scores are a measure of conservation, we can compare the distribution of phastCons scores in the *D. melanogaster* reference genome to the distribution of scores in sites harboring rare polymorphisms. Compared to common polymorphisms, the rarest frequency classes indeed have a distribution of phastCons scores closer to the neutral expectation (Supplemental Fig S6, $p < 2 \times 10^{-16}$, bootstrap KS test of whether singletons' phastCons CDF lies below the common polymorphisms' phastCons CDF).



Supplemental Fig S7: The fraction nonsynonymous (left) and nonsense (right) alleles present in heterozygous sites in the DGN. 'hetSingletons_conf' indicates a DGN singleton (frequency $\sim 1/621$) which was called as a heterozygote in DGN and confirmed heterozygous in the resequence data. 'het_conf_neverHomo' indicates all DGN polymorphisms (any frequency) which were called heterozygous in the DGN and also resequence data, and additionally were never found in a homozygous state in the DGN data. 'het_conf' indicates all DGN polymorphisms (any frequency) which were called heterozygous in DGN and also in the resequence data.



Supplemental Fig S8: The predicted GC equilibrium (as calculated from MA mutations and DGN polymorphisms, y-axis) is correlated with the actual GC content of the reference genome (as calculated or the center base pair for each neighbor context, x-axis)



Supplemental Fig S9: The six relative rates for MA, rare polymorphisms, and common polymorphisms, using all (A) non-repetitive regions, and (B) coding regions. The six relative rates metric is sensitive to the sequence content of the reference genome, and so when working with rare polymorphisms for this metric, we prefer to work with coding regions. This is a result of observing the reduced confirmation rate of singletons within introns, intergenic regions, and near indels, emphasizing the difficulty of validating rare polymorphisms within low-complexity regions. It has been found before that artifactual variant calls in high-coverage sequencing samples are largely driven by alignment errors [Li 2014]. This is worrisome when testing for mutational biases in the genome, because some tests rely inherently on our ability to ‘count the reference’, meaning accurately quantifying the relative proportions of different sequence contexts within the reference genome. For example, it is known that both AT-rich and GC-rich genomic regions are underrepresented in sequencing data [Dohm et al. 2008; Benjamini and Speed 2012], such that the GC-balanced regions of the genome with better read coverage may have a higher discovery rate of genetic variants. Therefore, even when we are confident our genotype calls are real, when working with rare polymorphisms we must be careful not to confound intrinsic rates of detection with intrinsic rates of mutation.

REFERENCES

Line	Generation sequenced	Total # mutations	chr2L count	chr2R count	chr3L count	chr3R count
MA_6	36	17	5	0	5	7
MA_9	36	15	3	3	4	5
MA_11	36	11	4	2	1	4
MA_14	49	32	9	5	7	11
MA_16	53	27	7	5	9	6
MA_17	37	14	3	4	4	3
MA_20	53	21	5	4	5	7
MA_21	53	27	3	9	7	8
MA_22	36	15	7	0	2	6
MA_24	36	19	13	1	3	2
MA_27	36	14	3	2	3	6
MA_28	36	10	1	6	3	0
MA_29	53	21	8	3	6	4
MA_30	53	21	2	7	2	10
MA_33	53	28	7	1	12	8
MA_35	53	15	1	4	4	6
MA_50	53	18	5	3	6	4

Supplemental Table S1: A summary of the strains sequenced in this study, including the generation at which each strain was sequenced, and the number of mutations identified for each strain.

REFERENCES

CHROM	POS	ID	REF	ALT	QUAL	FILTER	SAMPLEID	MutType	Result of Sanger sequencing	Forward primer	Reverse primer
2R	11218038		T A	PASS	MA_20			A->T/T->A	HET_ALTERNATE	GTGGAAGTTGGGGCTTTTAGG	AATACCCTTTGTGATGTCGGC
3L	16309582		A C	PASS	MA_28			A->C/T->G	HET_ALTERNATE	TTAGGCTTGGTTCGTGAC	TCCTCTTTGCCAATTGCTCG
3R	18719535		G T	PASS	MA_50			C->A/G->T	HET_ALTERNATE	GCGGAGTGACGAGAAAAATCA	CCAACCATCGCACTTCTGT
3R	2347435		G T	PASS	MA_33			C->A/G->T	HET_ALTERNATE	GGCTCGTGAATCATGCAGC	AAGTTGGTCCCTTTCGAGCC
3R	26031464		T A	PASS	MA_20			A->T/T->A	HET_ALTERNATE	CCCGAACTTAAAGCCATTCGTG	TAGTGCATTCTGCTCCGTT
3R	9439983		G A	PASS	MA_9			C->T/G->A	HET_ALTERNATE	TGCATAGATACAGCTCACGGAA	GGCAACTCAACGCAITCAAG
2R	3591057		G A	PASS	MA_21			C->T/G->A	HET_ALTERNATE	CTCCTTCTGGACCGACACC	ACAGGATGGAGACATCGGGA
2L	12926693		G C	PASS	MA_14			C->G/G->C	HET_ALTERNATE	TAATGCTGCAGCCAGCTCTC	GCTCGGGCAGTCTAAAAA
3L	23323893		T A	PASS	MA_6			A->T/T->A	HET_ALTERNATE	TGGAACGTGGACGTTTCTAGT	TCGGTCGAAAACAACCTCTCC
2R	13048443		T C	PASS	MA_27			A->G/T->C	HET_ALTERNATE	CTTAATGTTCCGTGTGCCCG	TTTTGGGGCAACAGGAGGAG
2L	22084319		C T	PASS	MA_24			C->T/G->A	HET_ALTERNATE	ACATGCATTCAAATGTTTCGGCT	TGAATGAAGTGGCAATGGGC
3R	6901818		T C	PASS	MA_30			A->G/T->C	HET_ALTERNATE	CAACCATGAACTGGTCTACTC	CGCGCAGCGAAAAAGTATT
3R	10076347		A G	PASS	MA_22			A->G/T->C	HET_ALTERNATE	AGGCAACAAAAATGCAGCCAA	TGTTGCTCGAAAAGAGGGCT
2R	2404216		G C	PASS	MA_17			C->G/G->C	HET_ALTERNATE	TCGAAGTATCAGTTGGGACA	CGCCAGTCAATTGCATATCCG
2L	3941683		T C	PASS	MA_9			A->G/T->C	HET_ALTERNATE	CTTAAAGCGAAAACCGTGGC	GTATCTTTCAGCCACCACAACG
3R	27703360		G C	PASS	MA_33			C->G/G->C	HET_ALTERNATE	ACTTGACAGTTACCAATGTAGCA	TGGCCATGACACAGGAAG
2R	10415065		C G	PASS	MA_29			C->G/G->C	HET_ALTERNATE	CCCCAGACACAAAAACTGGC	AAGTCGTCGTCAACCGCT
3R	6014803		A C	PASS	MA_14			A->C/T->G	HET_ALTERNATE	ACCCGCTGTTATGATCGCTT	TGGATGGCACCATCCGAACA
3R	12797570		G C	PASS	MA_30			C->G/G->C	HET_ALTERNATE	TGACACACCTACACACGCAA	TCAAGATGCGCTCTTAGCCC
3R	18153058		A G	PASS	MA_22			A->G/T->C	HET_ALTERNATE	ATTGCGCTGGCACTCGAATCA	GCCAGACCAATTGACTGCAT
2L	3901983		C G	PASS	MA_14			C->G/G->C	HET_ALTERNATE	ACTTGGCTGGGGCTCATAAC	AATGCAAGTGGCAATGCTG
3L	20694714		C T	PASS	MA_11			C->T/G->A	HET_ALTERNATE	CACGCTTAAAGTGGCACCTC	ACGTGAGTTGCGAAACAGAT
3R	24966148		C G	PASS	MA_30			C->G/G->C	HET_ALTERNATE	CGCCATATGCTGACACATCG	TACAGAAGTCAACCCCGTCG
2R	16989325		G C	PASS	MA_28			C->G/G->C	HOMO_REF	ATGGAAGAGGAAGCAGCCAC	ACAGAAAGCCGCAACTCAGG
3L	523073		C T	PASS	MA_14			C->T/G->A	HET_ALTERNATE	CCCATCACCACTGCTCGTAA	ATTTCTGTTTGCCAAAGGAGGC
3R	6627465		G T	PASS	MA_27			C->A/G->T	HET_ALTERNATE	TGCTGCAGCTGCTTCAAAT	GGGATATCTGTTACCGAAGAGCC
3R	3431114		G C	PASS	MA_20			C->G/G->C	HET_ALTERNATE	CTTACGTAAGTCTGCTCGTCA	AATCCGAGATGGAAGGACGC
3R	1709635		T C	PASS	MA_21			A->G/T->C	HET_ALTERNATE	CACACTGAAATGCAGCCAC	CACCGAAAACAGGATGGT
2L	12356513		T A	PASS	MA_16			A->T/T->A	HET_ALTERNATE	AGGTCAAGTATCTGATTGTCA	TTCCGGACATATCTGAGGT
3R	6727182		C T	PASS	MA_33			C->T/G->A	HET_ALTERNATE	CGTCCGCGGTTTAAAGAAC	AGACCTACGAGTATAAACCACT

Supplemental Table S3: A summary of the 30 mutations chosen randomly from our MA experiment for validation via PCR/Sanger sequencing. This resulted in either a double peak including the reference and alternate allele ('HET_ALTERNATE') which validates the new mutation, or a single peak matching the reference allele ('HOMO_REF') which is inconclusive.

REFERENCES

Study	MA method	# Lines	Generations per line (approx.)	Mutation count (filtered)	Mutation count (all)	Mutation rate	Chrom. used	Approx. genome length (bp)
MA combined	-	158	-	2141	3220	-	-	-
Assaf 2017	heterozygous	17	45	325	325	4.90E-09 (4.4-5.5e-9)	2,3	8.67E+07
Sharp 2016	heterozygous	112	60	740	786	6.03E-09 (5.6-6.5e-9)	2	1.94E+07
Huang 2016	hybrid	22	52	772	1036	5.21E-09 (4.9-5.5e-9 inferred)	X,2,3,4	1.74E+08
Schrider 2013	homozygous	4	145	164	218	3.27E-09 (2.85-3.73e-09)	X,2,3	1.15E+08
Keightley 2009	homozygous	3	262	140	174	3.46E-09 (2.96-4.01e-09)	X,2,3,4	6.40E+07
Other lines:								
Huang (mutator)	-	1	-	128	167	~20.00E-09 (17.0-23.3e-09 inferred)	-	1.57E+08
Schrider (mutator)	-	4	-	408	514	7.71E-09 (7.06-8.40e-09)	-	1.15E+08

Supplemental Table S4: A version of Table 1, with two extra columns indicating the chromosomes used in the experiment, and the back calculated genome length (lengths which were not consistently published within the MA papers). These were used for calculating a time base in the poisson exact test comparing the different single base pair mutation rates across experiments, and were found as follows: given that mutation rate $\mu = m/(n \times t \times l)$ (where m =mutation count, n =number of strains, t = number of generations, and l = number of base pairs), we back-calculated l .

Experiment	A → C/T → G	A → G/T → C	A → T/T → A	C → A/G → T	C → G/G → C	C → T/G → A
MA combined	0.06 (0.05-0.07)	0.11 (0.1-0.12)	0.12 (0.11-0.13)	0.18 (0.16-0.2)	0.13 (0.12-0.15)	0.4 (0.38-0.42)
Assaf 2016	0.04 (0.02-0.07)	0.14 (0.1-0.17)	0.13 (0.1-0.16)	0.19 (0.15-0.23)	0.16 (0.12-0.2)	0.34 (0.29-0.4)
Sharp 2016	0.06 (0.04-0.07)	0.11 (0.09-0.13)	0.12 (0.1-0.14)	0.18 (0.15-0.21)	0.1 (0.08-0.12)	0.44 (0.41-0.48)
Huang 2016	0.06 (0.04-0.07)	0.09 (0.07-0.11)	0.11 (0.09-0.13)	0.18 (0.15-0.21)	0.16 (0.13-0.19)	0.4 (0.37-0.44)
Schrider 2013	0.08 (0.04-0.12)	0.15 (0.1-0.2)	0.14 (0.1-0.2)	0.19 (0.13-0.25)	0.1 (0.05-0.14)	0.34 (0.27-0.41)
Keightley 2009	0.11 (0.06-0.16)	0.14 (0.1-0.21)	0.1 (0.05-0.15)	0.18 (0.11-0.24)	0.1 (0.06-0.16)	0.37 (0.29-0.45)
Other lines:						
Huang (mutator)	0.04 (0.01-0.07)	0.21 (0.15-0.29)	0.05 (0.01-0.08)	0.19 (0.12-0.26)	0.04 (0.01-0.08)	0.47 (0.38-0.56)
Schrider (mutator)	0.04 (0.02-0.05)	0.08 (0.06-0.11)	0.08 (0.05-0.1)	0.09 (0.07-0.12)	0.07 (0.05-0.1)	0.64 (0.59-0.68)

Supplemental Table S5: A summary of the six relative rates across the five MA studies, as well as a combined estimate. Note this is for the major autosomes 2 and 3 and with repeats masked. The 95% confidence intervals are within the parentheses, and were calculated using 1000 bootstraps of the raw counts.

REFERENCES

ALTCOUNT	tripCombo	C->A/G->T	C->G/G->C	C->T/G->A	GtestPvalue	pCORR	pSIG
MAcombined	ACA/TGT	18	27	51	4.00E-02	6.50E-01	FALSE
MAcombined	ACC/GGT	14	11	31	9.70E-01	1.50E+01	FALSE
MAcombined	ACG/CGT	11	9	42	1.70E-01	2.70E+00	FALSE
MAcombined	ACT/AGT	20	18	45	7.30E-01	1.20E+01	FALSE
MAcombined	AGA/TCT	26	23	49	3.60E-01	5.80E+00	FALSE
MAcombined	AGC/GCT	29	26	49	1.30E-01	2.00E+00	FALSE
MAcombined	AGG/CCT	17	13	38	9.80E-01	1.60E+01	FALSE
MAcombined	CCA/TGG	41	11	71	6.80E-03	1.10E-01	FALSE
MAcombined	CCC/GGG	19	10	44	5.60E-01	9.00E+00	FALSE
MAcombined	CCG/CGG	23	6	34	5.30E-02	8.40E-01	FALSE
MAcombined	CGA/TCG	17	13	49	5.60E-01	9.00E+00	FALSE
MAcombined	CGC/GCG	15	16	36	5.00E-01	8.00E+00	FALSE
MAcombined	GCA/TGC	40	19	53	5.50E-02	8.80E-01	FALSE
MAcombined	GCC/GGC	22	11	52	4.00E-01	6.30E+00	FALSE
MAcombined	GGA/TCC	15	21	67	2.50E-02	4.00E-01	FALSE
MAcombined	TCA/TGA	29	21	72	8.20E-01	1.30E+01	FALSE
MAcombined	AAA/TTT	29	21	44	1.90E-03	3.00E-02	FALSE
MAcombined	AAC/GTT	7	18	21	6.20E-01	9.80E+00	FALSE
MAcombined	AAG/CTT	10	23	28	6.20E-01	9.90E+00	FALSE
MAcombined	AAT/ATT	7	16	25	2.60E-01	4.20E+00	FALSE
MAcombined	ATA/TAT	11	20	13	3.00E-01	4.80E+00	FALSE
MAcombined	ATC/GAT	6	14	16	8.20E-01	1.30E+01	FALSE
MAcombined	ATG/CAT	3	19	22	3.70E-02	6.00E-01	FALSE
MAcombined	CAA/TTG	13	26	14	9.00E-02	1.40E+00	FALSE
MAcombined	CAC/GTG	8	15	9	3.30E-01	5.30E+00	FALSE
MAcombined	CAG/CTG	8	12	24	1.60E-01	2.60E+00	FALSE
MAcombined	CTA/TAG	7	19	14	5.20E-01	8.40E+00	FALSE
MAcombined	CTC/GAG	6	17	11	4.00E-01	6.40E+00	FALSE
MAcombined	GAA/TTC	12	11	14	2.20E-01	3.50E+00	FALSE
MAcombined	GAC/GTC	6	22	14	1.90E-01	3.00E+00	FALSE
MAcombined	GTA/TAC	6	17	8	1.50E-01	2.30E+00	FALSE
MAcombined	TAA/TTA	14	17	26	3.70E-01	6.00E+00	FALSE

Supplemental Table S6: The results of G tests for triplet effect on the mutation spectrum, here for the MA combined dataset. From left to right the columns refer to: variant dataset, triplet of interest (forward/reverse), mutation type 1, mutation type 2, mutation type 3, p value for G goodness of fit test (expected is total counts), corrected p value, and whether there is a significant effect of the triplet (p<0.01)

Mutation Class	Mutation Class Rate
A >C/T >G	4.50e-10
A >G/T >C	1.40e-09
A >T/T >A	1.32e-09
C >A/G >T	1.96e-09
C >G/G >C	1.64e-09
C >T/G >A	3.57e-09

Supplemental Table S7: The absolute mutation rates for each mutation type from Assaf et. al. 2017 (where the denominator for G:C base pairs is 28606251400 and the denominator for A:T base pairs is 37787276468. This comes from a total of 762 generations across all lines and a total of 87130614 base pairs of masked chromosomes 2 and 3, where 43.09% of these masked chromosomes consists of G:C base pairs)

REFERENCES

	Highly conserved sites (i.e. phastCons = 1)	Common variants (i.e. frequency 0.2-0.5)	Rare variants (i.e. singletons)
GO test	over-representation	under-representation	under-representation
Interpretation of GO test	This reveals which functions tend to be highly conserved	This reveals which functions are depleted of common polymorphisms, suggesting new mutations tend to be weakly to strongly deleterious	This reveals which functions are depleted of rare variants, suggesting new mutations tend to be strongly deleterious
GO categories discovered	chromatin assembly or disassembly nucleosome nucleosome assembly protein heterodimerization activity cytosol DNA binding translation triplet codon-amino acid adaptor activity ATP binding cytoplasm microtubule associated complex neurogenesis nucleus plasma membrane protein binding regulation of transcription, DNA-templated transcription factor activity, sequence-specific DNA binding	chromatin assembly or disassembly nucleosome nucleosome assembly protein heterodimerization activity cytosol DNA binding translation triplet codon-amino acid adaptor activity GGC codon-amino acid adaptor activity heat shock-mediated polytene chromosome puffing	chromatin assembly or disassembly nucleosome nucleosome assembly protein heterodimerization activity

Supplemental Table S8: The results of a GO analysis of over-represented terms within conserved sites (phastCons=1), under-represented terms within sites containing common polymorphisms (frequency 0.2-0.5), and under-represented terms with sites containing rare polymorphisms (frequency $\sim 1/621$). See Methods for more detail on analysis.

REFERENCES

ALTCOUNT	tripCombo	C->A/G->T	C->G/G->C	C->T/G->A	GtestPvalue	pCORR	pSIG
1	ACA/TGT	962	557	1740	2.20E-02	3.50E-01	FALSE
1	ACC/GGT	538	293	952	3.50E-01	5.60E+00	FALSE
1	ACG/CGT	515	211	973	2.40E-03	3.90E-02	FALSE
1	ACT/AGT	670	421	1238	1.60E-03	2.60E-02	FALSE
1	AGA/TCT	754	455	1471	2.70E-02	4.40E-01	FALSE
1	AGC/GCT	924	469	1430	5.10E-05	8.20E-04	TRUE
1	AGG/CCT	680	321	1045	1.40E-03	2.20E-02	FALSE
1	CCA/TGG	1032	398	1538	2.00E-08	3.20E-07	TRUE
1	CCC/GGG	669	297	1111	5.00E-02	8.00E-01	FALSE
1	CCG/CGG	557	249	965	1.70E-01	2.80E+00	FALSE
1	CGA/TCG	492	302	1431	6.80E-20	1.10E-18	TRUE
1	CGC/GCG	698	329	1203	3.00E-01	4.80E+00	FALSE
1	GCA/TGC	1183	483	1676	3.60E-11	5.80E-10	TRUE
1	GCC/GGC	813	512	1733	2.10E-04	3.30E-03	TRUE
1	GGA/TCC	553	389	1573	7.80E-19	1.20E-17	TRUE
1	TCA/TGA	829	415	1728	1.20E-03	1.90E-02	FALSE
1	AAA/TTT	676	833	1138	6.00E-31	9.60E-30	TRUE
1	AAC/GTT	348	890	801	4.10E-02	6.60E-01	FALSE
1	AAG/CTT	354	579	986	1.60E-23	2.50E-22	TRUE
1	AAT/ATT	381	817	986	4.70E-04	7.60E-03	TRUE
1	ATA/TAT	216	836	787	8.80E-13	1.40E-11	TRUE
1	ATC/GAT	158	602	444	1.20E-10	1.90E-09	TRUE
1	ATG/CAT	225	714	583	3.60E-06	5.80E-05	TRUE
1	CAA/TTG	432	654	607	4.30E-14	6.90E-13	TRUE
1	CAC/GTG	376	694	540	1.60E-11	2.60E-10	TRUE
1	CAG/CTG	274	493	665	2.30E-06	3.70E-05	TRUE
1	CTA/TAG	146	397	482	1.20E-04	2.00E-03	TRUE
1	CTC/GAG	177	492	415	1.10E-02	1.70E-01	FALSE
1	GAA/TTC	248	635	482	1.70E-05	2.70E-04	TRUE
1	GAC/GTC	157	690	365	4.00E-28	6.50E-27	TRUE
1	GTA/TAC	148	605	504	9.40E-11	1.50E-09	TRUE
1	TAA/TTA	327	634	842	7.40E-07	1.20E-05	TRUE

Supplemental Table S9: The results of G tests for triplet effect on the mutation spectrum, here for the singletons at frequency $\sim 1/621$. From left to right the columns refer to: variant dataset, triplet of interest (forward/reverse), mutation type 1, mutation type 2, mutation type 3, p value for G goodness of fit test (expected is total counts), corrected p value, and whether there is a significant effect of the triplet ($p < 0.01$)

REFERENCES

tripID	tripCombo	C->A/G->T	C->G/G->C	C->T/G->A	GtestPvalue	pCORR	pSIG
fourD	ACA/TGT	542	317	1614	9.40E-06	1.50E-04	TRUE
fourD	ACC/GGT	1557	989	2744	1.80E-37	3.00E-36	TRUE
fourD	ACG/CGT	853	515	1973	1.10E-01	1.80E+00	FALSE
fourD	ACT/AGT	626	447	2431	2.00E-26	3.20E-25	TRUE
fourD	AGA/TCT	428	276	1580	3.50E-16	5.70E-15	TRUE
fourD	AGC/GCT	436	284	2069	1.20E-49	1.90E-48	TRUE
fourD	AGG/CCT	866	555	2006	3.40E-02	5.50E-01	FALSE
fourD	CCA/TGG	1620	917	2693	1.00E-41	1.60E-40	TRUE
fourD	CCC/GGG	1338	844	2119	1.30E-50	2.10E-49	TRUE
fourD	CCG/CGG	1187	777	2754	3.60E-03	5.80E-02	FALSE
fourD	CGA/TCG	454	312	2016	8.40E-38	1.30E-36	TRUE
fourD	CGC/GCG	973	614	3095	2.00E-13	3.20E-12	TRUE
fourD	GCA/TGC	822	501	1930	2.30E-01	3.70E+00	FALSE
fourD	GCC/GGC	1195	767	2718	1.20E-03	1.90E-02	FALSE
fourD	GGA/TCC	906	558	2013	3.10E-03	5.00E-02	FALSE
fourD	TCA/TGA	588	408	2491	2.20E-39	3.40E-38	TRUE
fourD	AAA/TTT	143	364	201	9.20E-02	1.50E+00	FALSE
fourD	AAC/GTT	254	633	180	3.30E-28	5.20E-27	TRUE
fourD	AAG/CTT	233	464	450	5.10E-10	8.20E-09	TRUE
fourD	AAT/ATT	83	432	295	2.20E-09	3.60E-08	TRUE
fourD	ATA/TAT	67	323	144	2.40E-06	3.90E-05	TRUE
fourD	ATC/GAT	141	382	331	1.40E-04	2.20E-03	TRUE
fourD	ATG/CAT	93	460	185	6.80E-11	1.10E-09	TRUE
fourD	CAA/TTG	232	641	227	6.90E-16	1.10E-14	TRUE
fourD	CAC/GTG	354	1094	422	6.00E-19	9.50E-18	TRUE
fourD	CAG/CTG	407	942	689	3.00E-03	4.90E-02	FALSE
fourD	CTA/TAG	126	456	314	2.80E-03	4.50E-02	FALSE
fourD	CTC/GAG	451	729	948	4.80E-49	7.60E-48	TRUE
fourD	GAA/TTC	209	492	455	1.20E-07	1.90E-06	TRUE
fourD	GAC/GTC	423	1041	654	9.30E-02	1.50E+00	FALSE
fourD	GTA/TAC	111	502	188	3.60E-12	5.80E-11	TRUE
fourD	TAA/TTA	77	411	306	3.10E-11	5.00E-10	TRUE

Supplemental Table S10: The results of G tests for triplet effect on the substitution spectrum at four-fold degenerate sites. From left to right the columns refer to: evolved site dataset, triplet of interest (forward/reverse), mutation type 1, mutation type 2, mutation type 3, p value for G goodness of fit test (expected is total counts), corrected p value, and whether there is a significant effect of the triplet ($p < 0.01$)